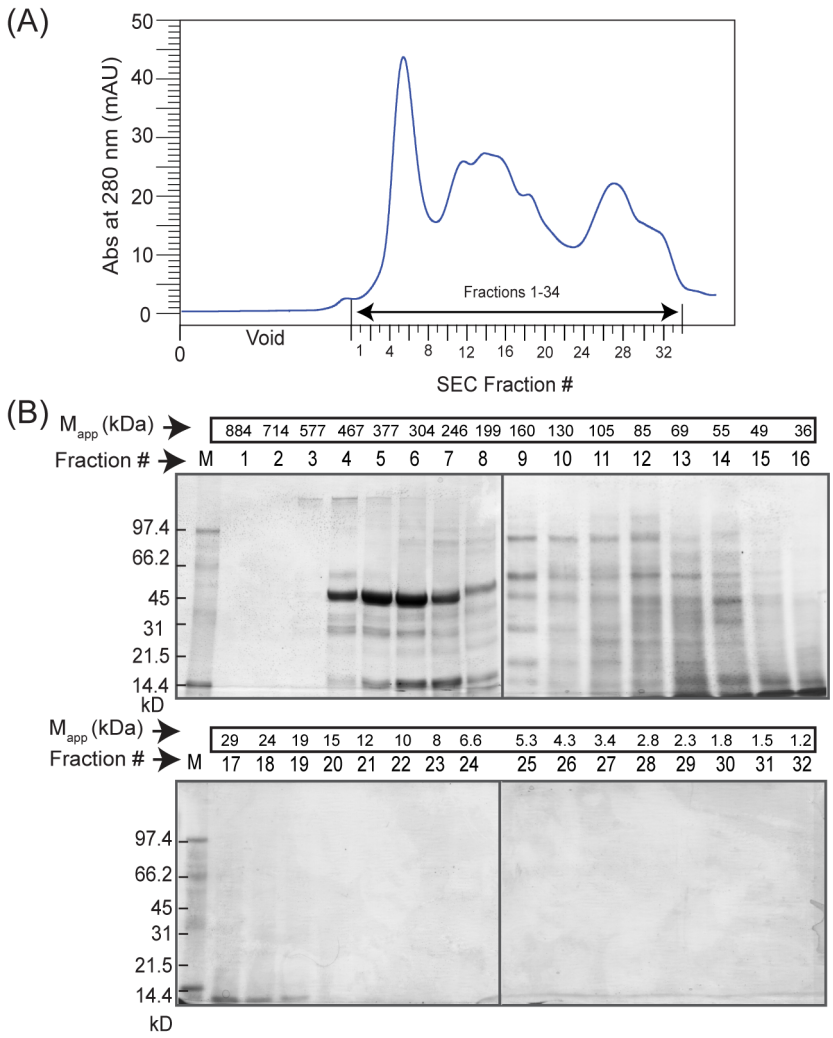

Supplemental Figure 1. SDS-PAGE analysis of SEC fractions obtained from leaf cytosol. (A) The UV chromatogram of biological replicate 2 showing profile of Arabidopsis leaf cytosol. Crude cytosol containing 1.5 mg protein was separated into 34 fractions of 0.5 ml each using Superdex 200 (300 mm × 10 mm) SEC column. Absorbance of eluted proteins was monitored at 280 nM as a function of fraction number. Fraction 1 is the void. Proteins in fractions 1-34 were subjected to LC-MS/MS analysis. Protein standards (669-29 kDa - thyroglobulin, apoferritin, β-amylase, alcohol dehydrogenase, bovine serum albumin and carbonic anhydrase) were used to generate a standard curve for calculation of apparent masse (M_{app}) of each identified protein. (B) SDS-PAGE separation of proteins in each SEC fraction. Equal volume (10 μl) of denatured and concentrated proteins from each fraction were resolved in 10% gels and stained with Coommassie blue. The M_{app} of proteins eluting in each fraction is shown on the top of each gel and was determined based on calibration equation generated based on the peak elution volume of the protein standards.

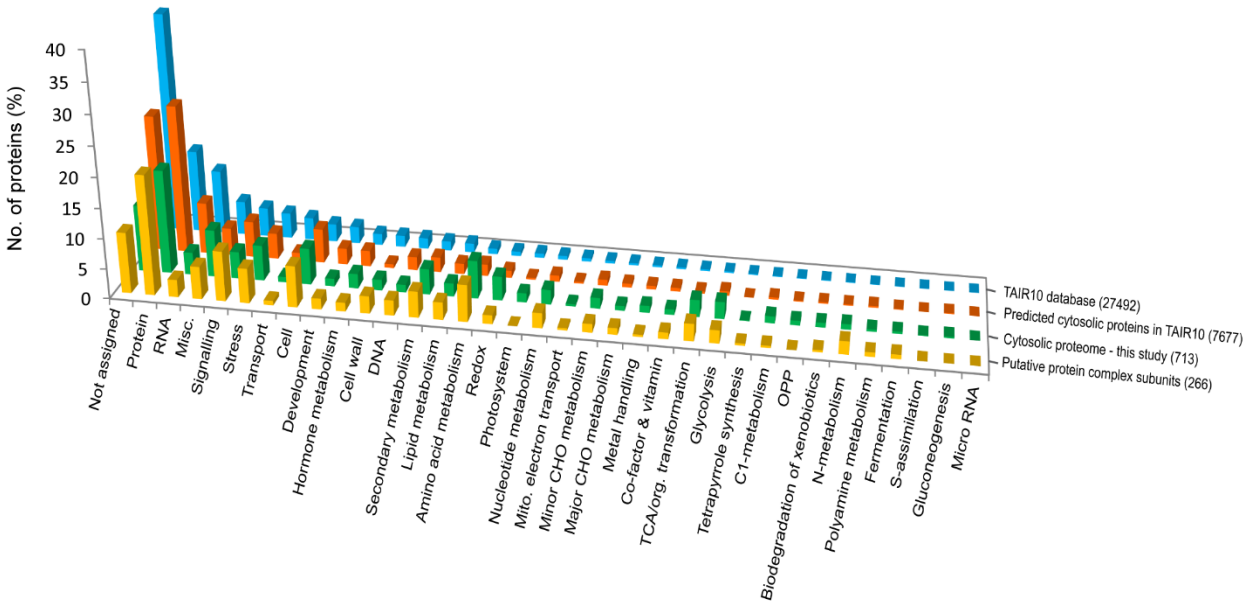

Supplemental Figure 2. Functional categories of total, predicted cytosolic proteins, and our experimentally analyzed cytosolic proteins. The 713 proteins that survived our filtering criteria including 266 putative protein complex subunits were analyzed for functions as outlined by MapMan code (Thimm et al., 2004) and compared with the putative cytosolic proteins from the TAIR10 protein database (7677 proteins) as well as the whole TAIR10 protein database. Putative cytosolic proteins in the whole TAIR10 database were predicted based on SUBA database (Heazlewood et al., 2007) followed by HMMTOP TMD prediction program (Tusnady and Simon, 1998) for any transmembrane domain containing proteins, and then TargetP analysis (Emanuelsson et al., 2007). The highest number of cytosolic proteins belong to protein synthesis, degradation, folding and post-translation modification which are grouped together as “protein”. Of 713 proteins, 78 were functionally unassigned or unknown, of which 29 are predicted to exist in protein complexes.

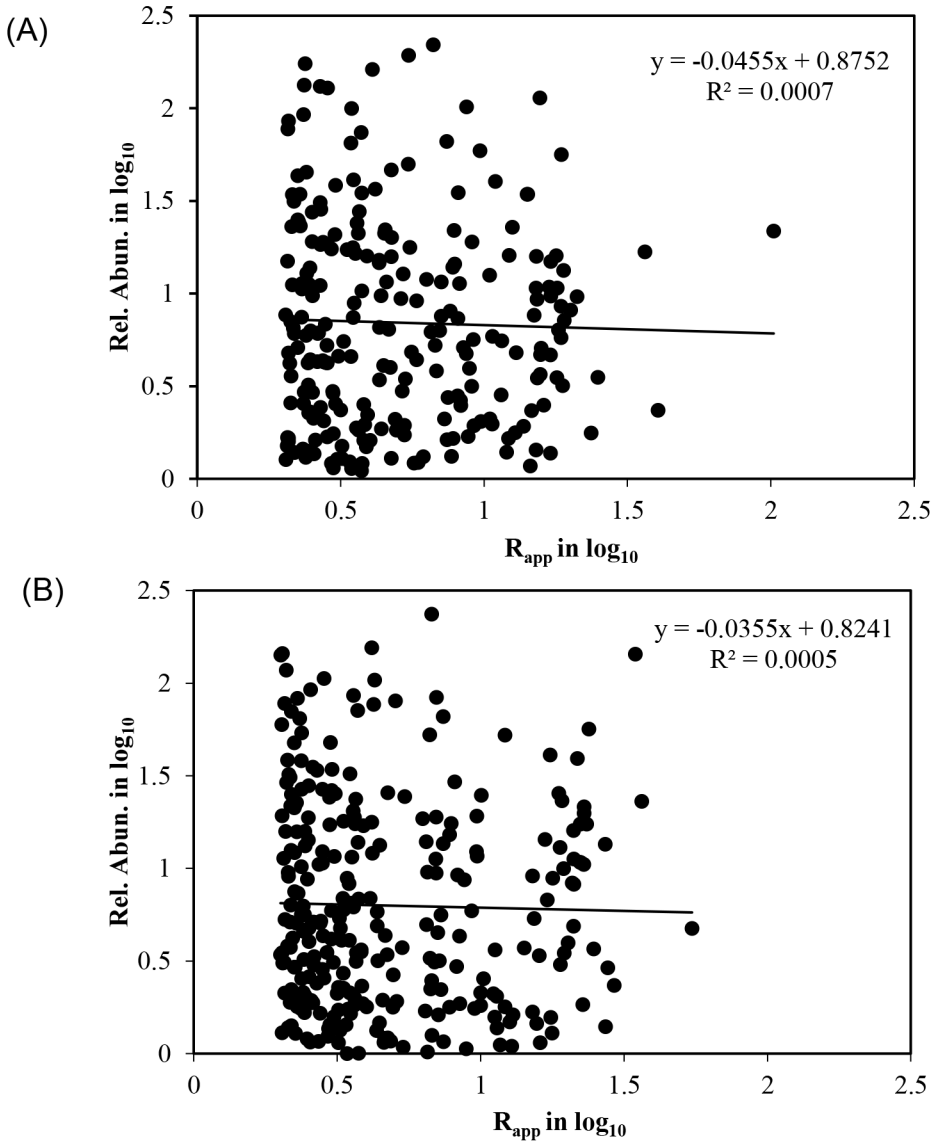

Supplemental Figure 3. Scatter plots of R_{app} and relative abundances of putative protein complexes in biological replicates 1 (A) and 2 (B). Data were plotted on a log scale. There was no correlation between relative abundance and likelihood of proteins complex formation. Rel. Abun., relative abundance.

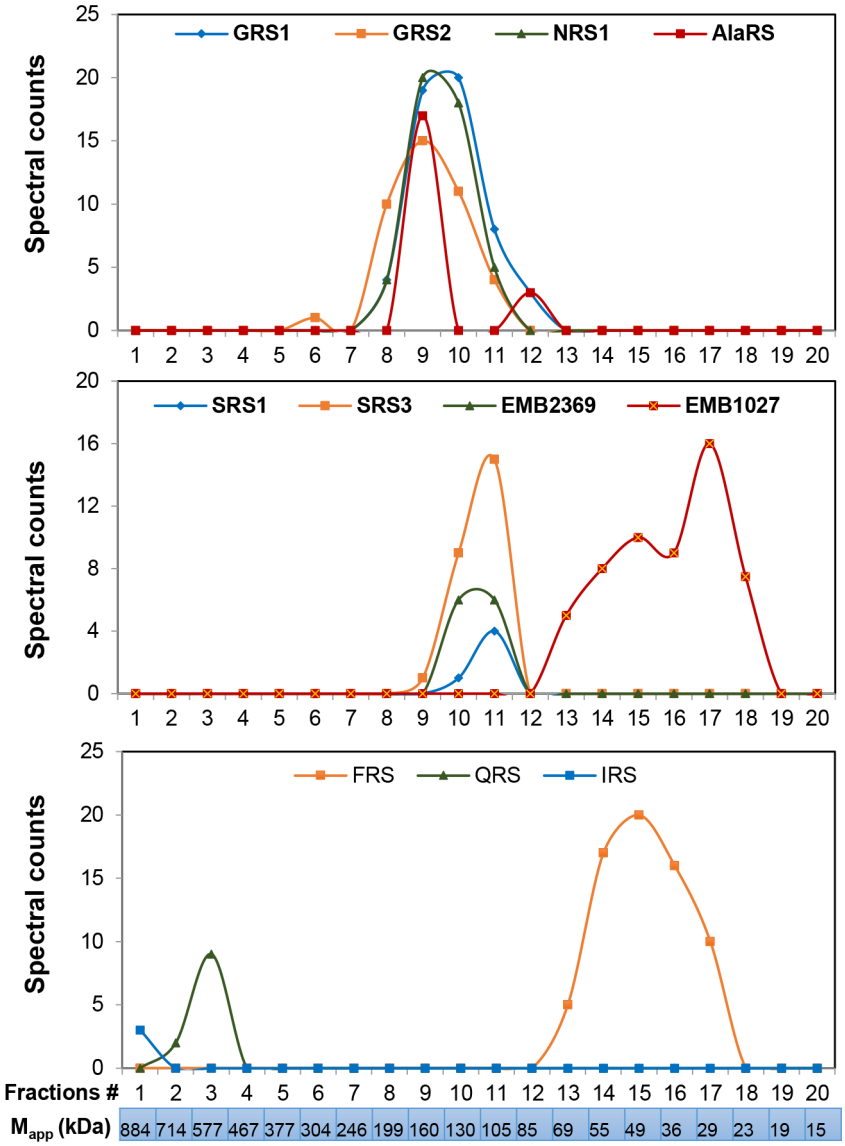

Supplemental Figure 4. Elution profiles of aminoacyl t-RNA synthetases. GRS1, *GLYCYL-tRNA SYNTHETASE1* (AT1G29880); GRS2, *GLYCYL-tRNA SYNTHETASE2* (AT3G48110); NRS1, *ASPARAGINYL*-tRNA *SYNTHETASE1* (AT5G56680); AlaRS, *ALANYL-tRNA SYNTHETASE* (AT1G50200); SRS1, *SERYL-tRNA SYNTHETASE1* (AT5G27470); SRS3, *SERYL-tRNA SYNTHETASE3*; EMB2369, *EMBRYO DEFECTIVE 2369* (AT4G04350); EMB1027, *EMBRYO DEFECTIVE 1027* (AT4G26300); FRS, *PHENYLALANYL-tRNA SYNTHETASE* (AT3G58140); QRS, *GLUTAMINYL-tRNA SYNTHETASE* (AT5G26710). The apparent mass of each SEC fraction is indicated below the x-axis. The elution profiles of IRS and QRS showed an obvious quaternary structure.

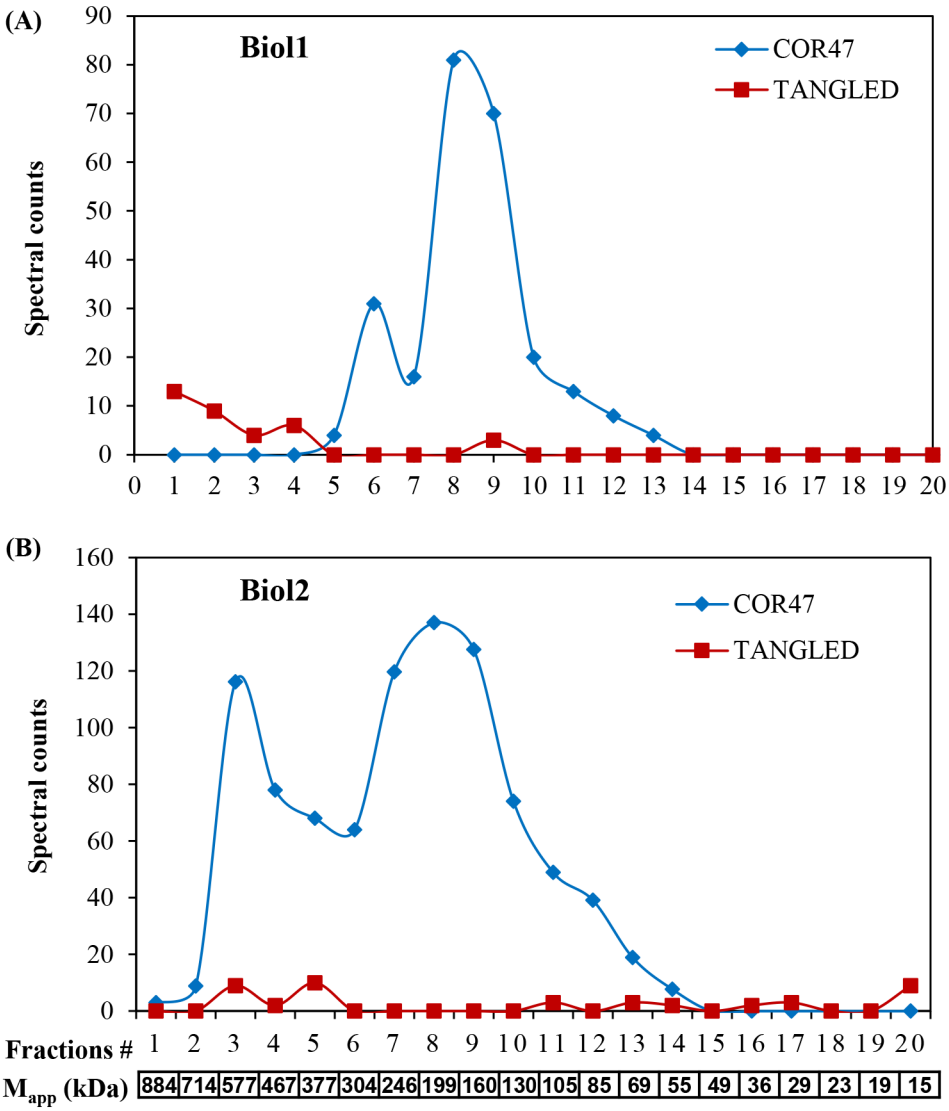

Supplemental Figure 5. Elution profiles of dehydrin COR47 (AT1G20440) and TANGLED (AT3G05330) on the SEC column in (A) biological replicate 1 and (B) biological replicate 2. The approximate mass of each SEC fraction is indicated below the x-axis. Both proteins were reproducibly identified as putative protein complexes.

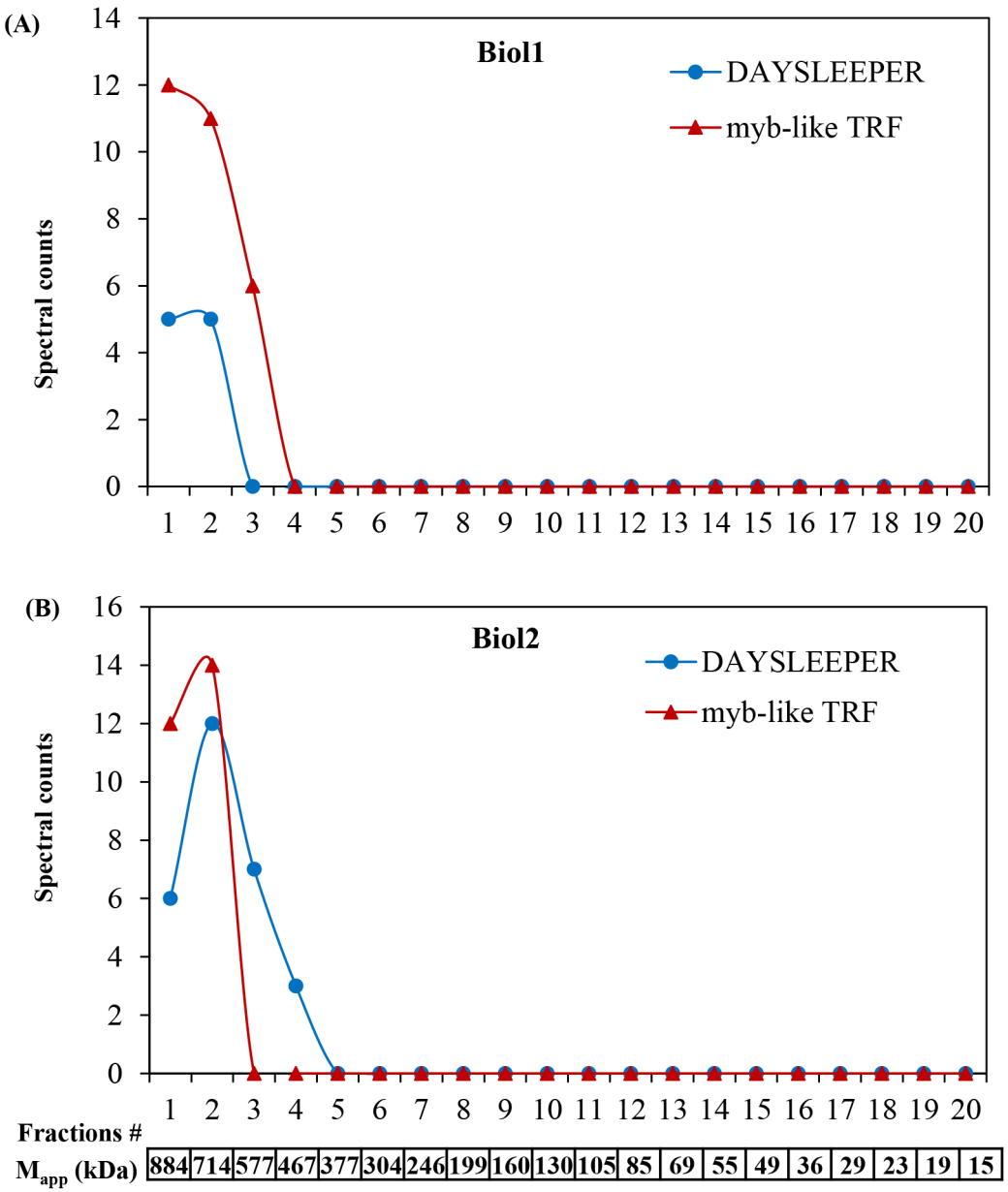

Supplemental Figure 6. Elution profiles of hAT-family transposase DAYSLEER (AT3G42170), and myb-like TRF transcription factor (AT1G58220) in (A) biological replicate 1 and (B) biological replicate 2. The approximate mass of each SEC fraction is indicated below the x-axis. Both proteins were reproducibly identified in higher mass fractions likely indicating their presence in large protein complexes.

SUPPLEMENTAL REFERENCES

Emanuelsson, O., Brunak, S., von Heijne, G., and Nielsen, H. (2007). Locating proteins in the cell using TargetP, SignalP and related tools. Nat Protoc *2*, 953-971.

Heazlewood, J.L., Verboom, R.E., Tonti-Filippini, J., Small, I., and Millar, A.H. (2007). SUBA: The Arabidopsis subcellular database. Nucleic Acids Res *35*, D213-D218.

Thimm, O., Blasing, O., Gibon, Y., Nagel, A., Meyer, S., Kruger, P., Selbig, J., Muller, L.A., Rhee, S.Y., and Stitt, M. (2004). MAPMAN: a user-driven tool to display genomics data sets onto diagrams of metabolic pathways and other biological processes. Plant J *37*, 914-939.

Tusnady, G.E., and Simon, I. (1998). Principles governing amino acid composition of integral membrane proteins: application to topology prediction. J Mol Biol *283*, 489-506.

Supplemental Table 1. Comparison of the apparent protein masses (M_{app}) determined from the current study with the published complex masses in the literature (M_{ref}) determined based on gel filtration chromatography. Biol1, biological replicate 1; Biol2, biological replicate 2; Ref.; references

Protein Name	Symbol	M_{mono} (kDa)	M_{app} (kDa) Biol1	M_{app} (kDa) Biol2	M_{ref} (kDa)	Organism	Ref.
Alcohol dehydrogenase	ADH (At1g77120)	41.8	84.9	84.9	80 (dimer)	Horse liver	[1]
Aldehyde dehydrogenase	ALDH (At3g48000)	58.9	199	161	200 (tetramer)	Arabidopsis	[2]
UDP-D xylose synthase	AXS1 (At1g08200), AXS2 (At1g08200)	44.2	105	105	91.6 (dimer)	Arabidopsis	[3]
UDP-D-galactose 4-epimerase 1	UGE1 (At1g12780)	39.4	68.7	68.7	83 (dimer)	Arabidopsis	[4]
Enolase	ENOC (At2g29560)	52	105	105	100 (dimer)	*Plasmodium falciparum*	[5]
Cytosolic enolase	ENO2 (At2g36530)	47.9	68.7	68.7	80 (dimer)	Human	[6]
PEP carboxylase	PEPC1 (At1g53310), PEPC3 (At3g14940	110	377	377	440 (tetramer)	*E. coli*	[7]
Glutamate decarboxylase	GAD5 (At3g17760)	56.2	130	304.9	115	*E. coli*	[8]
Aspartate aminotransferase	ASP3 (At5g11520)	49.1	84.9	84.9	92.7	Porcine heart	[9]
COP1-interactive protein 1	CIP1 (At5g41790)	182	714	884	700	Arabidopsis	[10]
Sucrose synthase	SUS1 (At5g20830)	92.3	246	246	360	Arabidopsis	[11]
Calmodulin 4	CAM4 (At1g66410)	17.8	44.8	44.8	36 (dimer)	Bovine	[12]
S-phase kinase-associated protein 1	SKP1 (At1g75950)	17.8	84.9	68.6	90.4	*E. coli*	[13]
Pyridoxine biosynthesis 1.1	PDX1:1 (At2g38230)	32.8	376.9	376.9	750	Arabidopsis	[14]
Glutamate decarboxylase 2	GAD2 (At1g65960)	56.1	129.9	160.8	140	Porcine brain	[15]
Acidic ribosomal family protein	At2g27710	11.4	68.6	84.9	~80 (pentamer)	Maize	[16]
ATP-citrate lyase	ACLB-1 (At3g06650); ACLB-2 (At5g49460)	65.8	466	577	550 (octamer)	Arabidopsis	[17]
Fructose bisphosphate aldolase	FBA6 At2g36460	38.4	130	130	~144 (tetramer)	Rabbit	[18]
Cytochrome C oxidase copper chaperone	Cox17 (At1g53030)	7.9	12.5	19.1	~16-32 dimer/tetramer	Yeast	[19, 19b]
Adenosine kinase	ADK1 (At3g09820) ADK2 (At5g03300)	37.8	84.8	84.8	~70 (dimer)	*Mycobacterium tuberculosis*	[20]
Beta carbonic anhydrase	BCA3 (At1g23730) BCA4 (At1g70410)	28.8	199	199	88 (tetramer)	*Clostridium perfringens*	[21]
Alanine:glyoxylate aminotransferase	AGT (At2g13360)	44.2	84.8	104.7	dimer	Yeast	[22]
Nitrilase	NIT1 (AT3G44310) NIT2 (AT3G44300) NIT3 (AT3G44320)	38.1	577	577	600 ultimeric)	*Aspergillus niger*	[23]
Nitrilase	NIT4 (At5g44300)	38.8	466	883	600 ultimeric)	*Aspergillus niger*	[23]
Cell division cycle 48	CDC48 (AT3G09840.1)	89.3	466	577	hexamer	Arabidopsis	[24]

Supplemental Table 1 References

1. **Hammes-Schiffer, S., and Benkovic, S. J.** (2009). Relating protein motion to catalysis. Ann. Rev. Biochem **75:** 519-41.
2. **Wei, Y., Lin, M., Oliver, D. J., and Schnable, P. S.** (2009). The roles of aldehyde dehydrogenases (ALDHs) in the PDH bypass of Arabidopsis. BMC Biochem. **10:** 7.
3. **Molhoj, M., Verma, R., and Reiter, W. D.** (2003). The biosynthesis of the branched-chain sugar d-apiose in plants: functional cloning and characterization of a UDP-d-apiose/UDP-d-xylose synthase from Arabidopsis. Plant J. **35:** 693-703.
4. **Barber, C., Rosti, J., Rawat, A., Findlay, K., Roberts, K., and Seifert, G. J.** (2006). Distinct properties of the five UDP-D-glucose/UDP-D-galactose 4-epimerase isoforms of Arabidopsis thaliana. J. Biol. Chem. **281:** 17276-85.
5. **Pal-Bhowmick, I., Sadagopan, K., Vora, H. K., Sehgal, A., Sharma, S., and Jarori, G. K.** (2004). Cloning, over-expression, purification and characterization of Plasmodium falciparum enolase. Eur. J. Biochem. **271:** 4845-4854.
6. **Pancholi, V.** (2001). Multifunctional alpha-enolase: its role in diseases. Cell. Mol. Life Sci. **58:** 902-20.
7. **O'Leary, B., Rao, S. K., Kim, J., and Plaxton, W. C.** (2009). Bacterial-type phosphoenolpyruvate carboxylase (PEPC) functions as a catalytic and regulatory subunit of the novel class-2 PEPC complex of vascular plants. J. Biol. Chem. **284:** 24797-805.
8. **Dutyshev, D. I., Darii, E. L., Fomenkova, N. P., Pechik, I. V., Polyakov, K. M., Nikonov, S. V., Andreeva, N. S., and Sukhareva, B. S.** (2005). Structure of Escherichia coli glutamate decarboxylase (GADalpha) in complex with glutarate at 2.05 angstroms resolution. Acta cryst. D. **61:** 230-5.
9. **Rhee, S., Silva, M. M., Hyde, C. C., Rogers, P. H., Metzler, C. M., Metzler, D. E., and Arnone, A**. (1997). Refinement and comparisons of the crystal structures of pig cytosolic aspartate aminotransferase and its complex with 2-methylaspartate. J. Biol. Chem. **272:** 17293-302.
10. **Zhu, D., Maier, A., Lee, J. H., Laubinger, S., Saijo, Y., Wang, H., Qu, L. J., Hoecker, U., and Deng, X. W.** (2008). Biochemical characterization of Arabidopsis complexes containing CONSTITUTIVELY PHOTOMORPHOGENIC1 and SUPPRESSOR OF PHYA proteins in light control of plant development. Plant Cell **20:** 2307-23.
11. **Zheng, Y.; Anderson, S.; Zhang, Y.; Garavito, R. M.** (2011). The structure of sucrose synthase-1 from Arabidopsis thaliana and its functional implications. J. Biol. Chem. **286:** 36108-18.
12. **Taketa, S., Barnes, J. A., Ubhi, M., and Sharma, R. K.** (1995). High molecular weight calmodulin-binding protein is phosphorylated by calmodulin-dependent protein kinase VI from bovine cardiac muscle. Mol. Cell. Biochem. **149-150:** 29-34.
13. **Hao, B., Oehlmann, S., Sowa, M. E., Harper, J. W., and Pavletich, N. P.** (2007). Structure of a Fbw7-Skp1-cyclin E complex: multisite-phosphorylated substrate recognition by SCF ubiquitin ligases. Mol. Cell **26:** 131-43.
14. **Leuendorf, J. E., Osorio, S., Szewczyk, A., Fernie, A. R., and Hellmann, H.** (2010). Complex assembly and metabolic profiling of Arabidopsis thaliana plants overexpressing vitamin B(6) biosynthesis proteins. Mol. Plant **3:** 890-903.
15. **Spink, D. C., Wu, S. J., and Martin, D. L.** (1991). Multiple forms of glutamate decarboxylase in porcine brain. J. Neurochem. **40**: 1113-9.
16. **Wool, I. G., Chan, Y. L., Gluck, A., and Suzuki, K.** (1991). The primary structure of rat ribosomal proteins P0, P1, and P2 and a proposal for a uniform nomenclature for mammalian and yeast ribosomal proteins. Biochim. **73:** 861-70.
17. **Fatland, B. L., Ke, J., Anderson, M. D., Mentzen, W. I., Cui, L. W., Allred, C. C., Johnston, J. L., Nikolau, B. J., and Wurtele, E. S.** (2002). Molecular characterization of a heteromeric ATP-citrate lyase that generates cytosolic acetyl-coenzyme A in Arabidopsis. Plant Physiol. **130:** 740-56.
18. **Sygusch, J., Beaudry, D., and Allaire, M.** (1987). Molecular architecture of rabbit skeletal muscle aldolase at 2.7-A resolution. PNAS USA **84:** 7846-50.
19. **(a) Heaton, D. N., George, G. N., Garrison, G., and Winge, D. R.** (2001). The mitochondrial copper metallochaperone Cox17 exists as an oligomeric, polycopper complex. Biochem. **40:** 743-51; (**b) Horng, Y. C., Cobine, P. A., Maxfield, A. B., Carr, H. S., and Winge, D. R.,** (2004). Specific copper transfer from the Cox17 metallochaperone to both Sco1 and Cox11 in the assembly of yeast cytochrome C oxidase. J. Biol. Chem. **279**: 35334-40.
20. **Long, M. C., Escuyer, V., and Parker, W. B.** (2003). Identification and characterization of a unique adenosine kinase from Mycobacterium tuberculosis. J. Bacteriol. **185:** 6548-55.
21. **Kumar, R. S., Hendrick, W., Correll, J. B., Patterson, A. D., Melville, S. B., and Ferry, J. G.** (2013). Biochemistry and Physiology of the beta Class Carbonic Anhydrase (Cpb) from Clostridium perfringens Strain 13. J. Bacteriol. **195:** 2262-9.
22. **Meyer, P., Liger, D., Leulliot, N., Quevillon-Cheruel, S., Zhou, C. Z., Borel, F., Ferrer, J. L., Poupon, A., Janin, J., and van Tilbeurgh, H.** (2005). Crystal structure and confirmation of the alanine:glyoxylate aminotransferase activity of the YFL030w yeast protein. Biochim. **87:** 1041-7.
23. **Kaplan, O., et al.** (2011). Heterologous expression, purification and characterization of nitrilase from Aspergillus niger K10. BMC Biotech. **11:** 2.
24. **Park, S., Rancour, D. M., and Bednarek, S. Y.** (2008). In planta analysis of the cell cycle-dependent localization of AtCDC48A and its critical roles in cell division, expansion, and differentiation. Plant Physiol. **148:** 246-58.

Supplemental Table 2. Proteins predicted to be subunits of large protein complexes with an R_{app} > 5 in both biological replicates.

Locus IDs	Protein names	Function	M_{mono} (kDa)	M_{app} Biol1 (kDa)	M_{app} Biol2 (kDa)	R_{app} Biol1	R_{app} Biol2	Rel. Abun. Biol1	Rel. Abun. Biol2
AT2G20140	AAA-type ATPase family protein	Protein degradation	49.3	714.0	577.0	14.5	11.70	1.2	1.1
AT5G16510	ALPHA-1,4-GLUCAN PROTEIN SYNTHASE	Cell wall synthesis	38.6	577.0	577.0	15.0	14.96	7.6	10.5
AT3G06650	ATP-CITRATE LYASE B-1 (ACLB-1)	TCA cycle	65.8	466.3	577.0	7.1	8.77	11.5	8.7
AT5G49460	ATP-CITRATE LYASE B-2 (ACLB-2)	TCA cycle	65.8	466.3	466.3	7.1	7.09	7.5	4.5
AT3G01500	BETA CARBONIC ANHYDRASE 1 (CA1)	Calvin cycle	29.5	160.8	198.9	5.5	6.75	193.3	235.3
AT5G14740	BETA CARBONIC ANHYDRASE 2 (CA2)	Calvin cycle	28.3	246.2	198.9	8.7	7.02	101.8	83.9
AT1G23730	BETA CARBONIC ANHYDRASE 3 (CA3)	Calvin cycle	28.8	160.8	198.9	5.6	6.90	4.8	3.1
AT1G70410	BETA CARBONIC ANHYDRASE 4 (CA4)	Calvin cycle	28.4	246.2	198.9	8.7	7.01	4.7	9.4
AT3G09840	CELL DIVISION CYCLE 48 (CDC48)	Cell division	89.3	466.3	577.0	5.2	6.46	12.8	13.9
AT1G14980	CHAPERONIN 10 (CPN10)	Protein folding	10.8	55.4	105.0	5.1	9.72	9.4	19.1
AT4G26780	Co-chaperone GrpE family protein (AR192)	Protein folding	36.1	304.6	304.6	8.4	8.44	4.7	4.8
AT1G20440	COLD-REGULATED 47 (COR47)	Stress response	29.9	198.9	198.9	6.7	6.66	220.5	52.5
AT5G52310	COLD-REGULATED 78 (COR78)	Stress response	77.8	577.0	577.0	7.4	7.42	66.3	66.0
AT3G23490	CYANASE (CYN)	Secondary metabolism	18.6	198.9	129.9	10.7	6.99	5.9	11.3
AT1G35580	CYTOSOLIC INVERTASE 1 (CINV1)	Major CHO metabolism	62.8	466.3	466.3	7.4	7.43	1.6	1.2
AT3G42170	DAYSLEEPER	DNA repair	78.8	714.0	883.5	9.1	11.22	3.2	1.6
AT1G20450	EARLY RESPONSIVE TO DEHYDRATION 10 (ERD10)	Stress response	29.5	160.8	160.8	5.4	5.44	50.0	24.4
AT1G20200	EMBRYO DEFECTIVE 2719 (emb2719)	Protein degradation	55.5	714.0	714.0	12.9	12.85	1.8	1.1
AT3G54400	Eukaryotic aspartyl protease family protein	RNA regulation	45.4	714.0	714.0	15.7	15.71	3.7	1.5
AT2G38590	F-box and associated interaction domains-containing	Protein degradation	50.3	376.9	883.5	7.5	17.56	2.8	1.6
AT2G36460	FRUCTOSE BISPHOSPHATE ALDOLASE 6	Glycolysis	38.4	714.0	466.3	18.6	12.16	56.3	52.4
AT5G37600	GLUTAMINE SYNTHASE (GLN1;1)	N-metabolism	39.1	246.2	304.6	6.3	7.79	11.9	15.2
AT1G66200	GLUTAMINE SYNTHASE (GLN1;2)	N-metabolism	39.2	304.6	246.2	7.8	6.28	13.9	18.6
AT3G17820	GLUTAMINE SYNTHASE (GLS1;3)	N-metabolism	38.6	304.6	246.2	7.9	6.38	14.5	17.5
AT5G26710	GLYTAMYL-tRNA SYNTHETASE (QRS)	Protein activation	81.0	714.0	577.0	8.8	7.12	1.7	1.6
AT4G15802	HEAT SHOCK FACTOR BINDING PROTEIN (HSBP)	Protein folding	9.3	84.9	105.0	9.1	11.24	19.0	3.6
AT3G23990	HEAT SHOCK PROTEIN 60 (HSP60)	Protein folding	61.2	577.0	577.0	9.4	9.42	5.7	8.8
AT2G33210	HEAT SHOCK PROTEIN 60-2 (HSP60-2)	Protein folding	61.9	714.0	577.0	11.5	9.32	5.6	5.9
AT4G22670	HSP70-INTERACTING PROTEIN 1 (HIP1)	Protein folding	46.6	304.6	304.6	6.5	6.54	6.2	9.5
AT1G58220	Homeodomain-like superfamily protein	RNA regulation	86.2	714.0	883.5	8.3	10.25	2.7	2.5
AT4G22485	Lipid-transfer family protein	Protease inhibitor	68.2	714.0	883.5	10.5	12.96	2.1	1.6

AT4G22505	Lipid-transfer family protein	Protease inhibitor	55.2	714.0	883.5	12.9	16.01	4.8	3.4
AT4G09620	Mitochondrial transcription termination factor	Unknown	24.0	198.9	160.8	8.3	6.70	2.5	2.2
AT1G18800	NAP1-RELATED PROTEIN 2 (NRP2)	DNA synthesis	29.5	198.9	198.9	6.8	6.75	5.3	2.5
AT3G05900	Neurofilament protein-related	Unknown	73.4	577.0	714.0	7.9	9.73	21.9	11.7
AT3G44310	NITRILASE 1 (NIT1)	Cyanide hydrolysis	38.1	466.3	714.0	12.2	18.73	16.0	25.4
AT3G44300	NITRILASE 2 (NIT2)	Cyanide hydrolysis	37.1	466.3	714.0	12.6	19.23	22.8	23.2
AT3G44320	NITRILASE 3 (NIT3)	Cyanide hydrolysis	38.0	577.0	577.0	15.2	15.19	10.7	9.1
AT5G22300	NITRILASE 4 (NIT4)	Cyanide hydrolysis	38.9	466.3	883.5	12.0	22.73	1.4	1.8
AT1G79210	Ntn-hydrolases superfamily protein	Protein degradation	25.7	376.9	577.0	14.7	22.44	2.3	10.7
AT3G26340	Ntn-hydrolases superfamily protein	Protein degradation	29.5	466.3	577.0	15.8	19.58	5.1	3.5
AT4G31300	Ntn-hydrolases superfamily protein (PBA1)	Protein degradation	25.1	466.3	577.0	18.6	22.96	8.5	19.9
AT3G60820	Ntn-hydrolases superfamily protein (PBF1)	Protein degradation	24.6	466.3	577.0	18.9	23.43	13.4	17.3
AT4G09320	NUCLEOSIDE DIPHOSPHATE KINASE 1 (NDPK1)	Nucleotide metabolism	18.8	376.9	466.3	20.0	24.80	8.1	3.7
AT2G42910	Phosphoribosyltransferase family protein	Nucleotide metabolism	37.5	714.0	577.0	19.0	15.37	7.2	5.4
AT3G06930	ARGININE METHYLTRANSFERASE 4B (PRMT4B0	Methyltransferase	59.7	466.3	466.3	7.8	7.81	1.6	1.8
AT2G38230	PYRIDOXINE BIOSYNTHESIS 1.1 (PDX1.1)	Co-factor synthesis	32.8	376.9	466.3	11.5	14.20	2.8	3.7
AT5G14800	PYRROLINE-5-CARBOXYLATE	Amino acid metabolism	28.6	714.0	577.0	25.0	20.17	3.5	4.0
AT5G11580	RCC1 family protein	Cell division	60.5	466.3	577.0	7.7	9.54	1.3	1.8
AT5G01410	REDUCED SUGAR RESPONSE 4 (RSR4)	Co-factor synthesis	33.2	304.6	246.2	9.2	7.42	5.6	13.6
AT3G05530	REGULATORY PARTICLE TRIPLE-A ATPASE 5A (RPT5A)	Protein degradation	47.5	577.0	577.0	12.2	12.16	1.7	1.8
AT5G15650	REVERSIBLY GLYCOSYLATED POLYPEPTIDE 1 (RGP1)	Cell wall synthesis	40.9	577.0	714.0	14.1	17.47	34.3	40.9
AT3G02230	REVERSIBLY GLYCOSYLATED POLYPEPTIDE 1 (RGP2)	Cell wall synthesis	40.6	577.0	883.5	14.2	21.76	34.4	39.2
AT5G50750	REVERSIBLY GLYCOSYLATED POLYPEPTIDE 4 (RGP4)	Cell wall synthesis	41.8	714.0	714.0	17.1	17.07	4.7	6.7
AT1G23410	RIBOSOMAL PROTEIN S27A	Protein synthesis	17.7	714.0	714.0	40.4	40.43	2.3	7.2
AT3G13570	SC35-LIKE SPLICING FACTOR 30A (SCL30A)	RNA processing	30.2	714.0	883.5	23.6	29.25	1.8	2.3
AT4G37930	SERINE TRANSHYDROXYMETHYLTRANSFERASE (SHMT1)	C1-metabolism	57.4	466.3	466.3	8.1	8.13	35.1	29.3
AT3G15390	SILENCING DEFECTIVE 5 (SDE5)	RNA transcription	55.1	466.3	466.3	8.5	8.46	5.1	1.9
AT3G05330	TANGLED	Cell cycle	49.5	376.9	883.5	7.6	17.85	8.0	8.8
AT1G72050	TRANSCRIPTION FACTOR IIIA (TFIIIA)	rRNA transcription	46.6	376.9	466.3	8.1	10.00	2.8	1.8
AT1G30230	TRANSLATION ELONGATION FACTOR 1B BETA (EF1B-B1)	Protein synthesis	25.1	466.3	466.3	18.6	18.57	5.8	21.5
AT5G12110	TRANSLATION ELONGATION FACTOR 1B GAMMA (EF1B-B2)	Protein synthesis	24.8	376.9	160.8	15.2	6.49	15.9	5.0
AT1G09640	TRANSLATION ELONGATION FACTOR 1B GAMMA (EF1B-G1)	Protein synthesis	46.6	246.2	466.3	5.3	10.00	1.7	2.1
AT2G40660	Nucleic acid-binding, OB-fold-like protein	Protein activation	42.1	577.0	466.3	13.7	11.09	1.9	2.1
AT4G10320	tRNA synthetase class I	Protein activation	135.4	714.0	883.5	5.3	6.53	1.9	1.0
AT5G23860	TUBULIN BETA 8 (TUB8)	Cell organization	50.6	466.3	577.0	9.2	11.41	1.9	1.4

AT5G48575	Unknown protein	Unknown	11.2	198.9	304.6	17.7	27.17	10.6	13.5
AT1G26921	Unknown protein	Unknown	5.6	105.0	304.6	18.8	54.52	3.2	4.7
AT1G62480	Vacuolar Ca-binding protein-related	Calcium signaling	16.6	160.8	160.8	9.7	9.67	58.9	12.3
AT1G12080	Vacuolar calcium-binding protein-related	Unknown	15.4	160.8	129.9	10.5	8.45	12.6	4.3
AT3G29340	Zinc finger (C2H2 type) family protein	RNA regulation	72.7	376.9	466.3	5.2	6.41	3.0	1.7
AT5G60160	Zn-dependent exopeptidases superfamily protein	Protein degradation	52.4	466.3	376.9	8.9	7.19	3.9	3.2

M_{mono}, predicted mass of monomers; M_{app}, apparent mass of complexes; R_{app}, the ratio of the M_{app} to the M_{mono}, Biol1, biological replicate 1; Biol2, biological replicate 2; Rel. Abun., relative abundance.